Biochimica et Biophysica Acta 1864 (2016) 1489–1499

Contents lists available at ScienceDirect

Biochimica et Biophysica Acta

journal homepage: www.elsevier.com/locate/bbapap

Structural model of amyloid fibrils for amyloidogenic peptide from Bgl2p–glucantransferase of *S. cerevisiae* cell wall and its modifying analog. New morphology of amyloid fibrils

Olga M. Selivanova [a], Anna V. Glyakina [a,b], Elena Yu. Gorbunova [c], Leila G. Mustaeva [c], Mariya Yu. Suvorina [a], Elizaveta I. Grigorashvili [a], Alexey D. Nikulin [a], Nikita V. Dovidchenko [a], Valentina V. Rekstina [d], Tatyana S. Kalebina [d], Alexey K. Surin [a,e], Oxana V. Galzitskaya [a,*]

[a] Institute of Protein Research, Russian Academy of Science, 142290 Pushchino, Moscow Region, Russia
[b] Institute of Mathematical Problems of Biology RAS, Keldysh Institute of Applied Mathematics of Russian Academy of Sciences, 142290 Pushchino, Moscow Region, Russia
[c] Branch of Federal State Budgetary Research Institution, "M.M. Shemyakin and Yu.A. Ovchinnikov Institute of Bioorganic Chemistry, Russian Academy of Sciences", Nauka Pr. 4, 142290 Pushchino, Moscow Region, Russia
[d] Department of Molecular Biology, Faculty of Biology, Moscow State University, Moscow, Russia
[e] State Research Center for Applied Microbiology & Biotechnology, Obolensk, Serpukhov District, Moscow Region 142279, Russia

ARTICLE INFO

Article history:
Received 13 May 2016
Received in revised form 21 July 2016
Accepted 3 August 2016
Available online 06 August 2016

Keywords:
Amyloid fibrils
Oligomer
Amyloidogenic regions
Tandem mass spectrometry
Molecular structure
Electron microscopy
X-ray analysis

ABSTRACT

We performed a comparative study of the process of amyloid formation by short homologous peptides with a substitution of aspartate for glutamate in position 2 – V**D**SWNVLVAG (AspNB) and V**E**SWNVLVAG (GluNB) – with unblocked termini. Peptide AspNB (residues 166–175) corresponded to the predicted amyloidogenic region of the protein glucantransferase Bgl2 from the *Saccharomyces cerevisiae* cell wall. The process of amyloid formation was monitored by fluorescence spectroscopy (FS), electron microscopy (EM), tandem mass spectrometry (TMS), and X-ray diffraction (XD) methods. The experimental study at pH 3.0 revealed formation of amyloid fibrils with similar morphology for both peptides. Moreover, we found that the morphology of fibrils made of untreated ammonia peptide is not mentioned in the literature. This morphology resembles snakes lying side by side in the form of a wave without intertwining. Irrespective of the way of the peptide preparation, the rate of fibril formation is higher for AspNB than for GluNB. However, preliminary treatment with ammonia highly affected fibril morphology especially for AspNB. Such treatment allowed us to obtain a lag period during the process of amyloid formation. It showed that the process was nucleation-dependent. With or without treatment, amyloid fibrils consisted of ring-like oligomers with the diameter of about 6 nm packed either directly ring-to-ring or ring-on-ring with a slight shift. We also proposed the molecular structure of amyloid fibrils for two studied peptides.

1. Introduction

The study of the process of amyloid formation is an important field of research on protein behavior. Many proteins and peptides capable of forming amyloids are associated with severe human neurodegenerative diseases such as Parkinson's and Alzheimer's disease and others. Amyloids are fibril formations generating deposits or amyloid plaques in different tissues of organisms [1]. The principal characteristic of amyloids is supposed to be the presence of a cross-β structure [2]. This structure can be revealed with the use of X-ray diffraction and reflects the specific organization of fibrils, where β-layers lying parallel to the fibril axis at a distance of 9–11 Å from each other consist of β-strands that are at a distance of 4.6–4.8 Å from each other and perpendicular to the fibril axis.

However, there are proteins and peptides that can form amyloids nontoxic for a human organism – functional amyloids [3,4]. Some human hormones exist for a long time as amyloid structures in secretory granules and can leave them as monomer molecules without losing their functional activity [5].

It has been shown earlier that one of the proteins from the *Saccharomyces cerevisiae* cell wall (glucantransferase Bgl2) forms amyloid structures after isolation from cell wall [6]. The pH-dependent capacity of this protein to form fibril structures was studied. The capacity of potentially

Abbreviations: "NB", unblocked peptide termini; Bgl2p, glucantransferase Bgl2p; ThT, thioflavin T; PAD, potential amyloidogenic determinant; FS, fluorescence spectroscopy; EM, electron microscopy; XD, X-ray diffraction; TMS, tandem mass spectrometry.

* Corresponding author at: Institute of Protein Research, Russian Academy of Sciences, Institutskaya Street 4, Pushchino, Moscow Region, Russia.
E-mail address: ogalzit@vega.protres.ru (O.V. Galzitskaya).

http://dx.doi.org/10.1016/j.bbapap.2016.08.002
1570-9639/

amyloidogenic regions (PADs) in the Bgl2p sequence to generate amyloid formation was examined using the bioinformatics analysis [7]. Short amyloidogenic regions of the sequence can be predicted in many proteins. The analysis of their capacity to form amyloids and understanding of the dependence of amyloid properties on different conditions (synthesis, pH, temperature, ionic strength, etc.) are important for the understanding of general mechanisms of amyloidogenesis in proteins. The tendency to form amyloids is frequently revealed with bioinformatics methods and is associated with self-recognition elements in the sequence [8]. Such elements of the primary structure constitute the backbone of amyloid fibrils [9,10] and are hot spots for aggregation of native proteins with the subsequent formation of amyloid fibrils [11]. These structures have typical characteristics of amyloids. 1) Morphology can be revealed in electron microscopes. Fibrils are highly elongated and mostly not branched protease-stable polymers up to 20 μm in length and from 2 to 20 nm in diameter in average. They consist of several filaments, which can be intertwined or packed in parallel. Moreover, morphological polymorphism of fibrils is frequently observed within the same sample. 2) Fibrils are capable of binding some stains (for example, ThT) with different intensity, which can be registered using fluorescence spectroscopy. 3) At last, the final answer to the question whether it is the amyloid or amyloid-like structure is obtained using the X-ray diffraction analysis. Most amyloids have the characteristic patterns of X-ray diffraction [2].

The existence of a cross-β structure was demonstrated for protein glucantransferase Bgl2p by the method of fluorescence spectroscopy with the use of thioflavin T and it was shown with the use of electron microscopy that the formed aggregates had a fibril structure [6].

A significant aspect of studying amyloid structures is determining conditions and factors that affect the process of amyloid formation, such as temperature, pH, ionic strength, the presence of ligands and others. A more challenging task is to identify amyloidogenic regions, which are critical to amyloid formation in a biological context, and to predict the effects of protein mutations and modifications on propensity to form amyloids in vivo. It is possible that in spite of a great variety of experimental data on this issue, there are general key mechanisms for all proteins. To exclude the effect of different contexts in proteins, small model peptides are used, the most part of their sequence being a priori the amyloidogenic region. For prediction of such regions different computation algorithms are used [12]. In our previous study we successfully used model peptides from Bgl2p to analyze the dependence of amyloid formation on pH values [7]. We examined the ability of peptides to form amyloid fibrils in the acidic pH range, since it was previously shown that Bgl2p is capable of forming fibrils at pH values below 6.0 [6]. It is known that the acid treatment of yeast cells leads to the occurrence of an apoptotic phenotype and induction of general stress response pathways that may include the mechanisms of cell wall integrity control [13–16]. It can be assumed that the ability to form fibrils facilitates yeast cell protection against oxidative stress.

To fully understand the mechanism of amyloidogenesis, it is necessary to know not only the reasons why proteins undergo these conformational changes, but also how these changes occur. It is believed that formation of amyloids goes through formation of a nucleus, to which other monomer molecules are attached later. We developed a model that makes it possible to estimate the size of an amyloid nucleus on the basis of kinetic data obtained with fluorescence spectroscopy [17]. For insulin and Aβ peptide the possible mechanism of amyloid formation was proposed: monomer → oligomer → amyloid fibril and it was demonstrated that the amyloid fibrils consist of oligomer structures [18–20].

In this study we analyzed the process of amyloid formation by the peptide that was predicted as a potentially amyloidogenic region of protein Bgl2p V**D**SWNVLVAG (residues 166–175) by using three programs: Aggrescan, DHPred, and FoldAmyloid. Other programs: PASTA, Tango and Waltz did not predict this region as an amyloidogenic one [7]. In addition to the mentioned peptide, we also synthesized a peptide with the Asp2Glu substitution. Using the methods of fluorescence spectroscopy, electron microscopy, tandem mass spectrometry and X-ray structural analysis, the characteristics of the aggregates obtained at pH 3.0 were analyzed and the dependence of amyloid formation on the peptide concentration in solution was studied. The comparison of the data, obtained for the two peptides, allowed us to conclude that substitutions of D for E affected the process of amyloid formation. Using the electron microscopy method, we also described new amyloid morphology not mentioned in the literature and presented the molecular structure of amyloid fibrils. We found that amyloid fibrils consisted of ring-like oligomer structures and possible mechanism of amyloid formation was proposed for the studied peptides.

2. Materials and methods

*2.1. Synthesis of peptides: V**D**SWNVLVAG (AspNB) and V**E**SWNVLVAG (GluNB)*

Peptides were obtained by solid-phase peptide synthesis. The strategy of the synthesis was based on the 9-fluorenylmethyloxycarbonyl/*t*-butyl ether (Fmoc/*t*Bu) protocol using an alkoxybenzyl alcohol resin as the solid phase. The following side-chain protecting groups were applied: *t*Bu (*tert*-butyl) for Asp, Glu and Ser, Trt (trityl) for Asn, Boc (*tert*-butyloxycarbonyl) for Trp. The first amino acid (Gly) was coupled with the polymer by dicyclohexylcarbodiimide (DCC) in the presence of 4-dimethylaminopyridine (DMAP). After attachment of the first amino acid, residual hydroxyl groups of the polymer were blocked by benzoyl chloride. All coupling reactions were performed step by step with the 2-(1-benzotriazole-1-yl)-1,1,3,3-tetramethyluronium tetrafluoroborate (TBTU) method, using a solution of 2.5 equivalents of each Fmoc-amino acid derivative in *N*-methylpyrrolidone (NMP). Double coupling of the Fmoc-amino acids was carried out to ensure the reaction completion, which was monitored at each stage using ninhydrin tests. The presence in a sequence of more than four hydrophobic residues requires increasing the time of reaction to 12 h and the number of couplings in succession. The peptides were detached from the polymer with a freshly prepared mixture of trifluoroacetic acid (TFA)-triisopropylsilane (TIS)-water (95:2.5:2.5) during 2 h under Ar. The resin was filtered and washed with TFA and dichloromethane. The peptides were precipitated using cold diethyl ether, dried and purified by reversed phase high performance liquid chromatography (RP-HPLC). Chromatography was carried out on a high pressure chromatograph (Waters with Waters 2487 Dual Absorbance Detector and Waters 1525 Binary HPLC Pump). Semipreparative purification was performed on a Diasorb 130 C16T 6 Å (250 × 8 mm) column in acetonitrile gradient in 0.1% TFA/water at a flow of 2 ml/min, the wave length of detection was 226 nm. The samples were dissolved in dimethylsulfoxide (DMSO) and applied on the column. Analytical HPLC was carried out on Luna 5u C18 (2) 100 Å (250 × 4.6 mm). The purity of the products was 99.8%. The molecular mass and homogeneity of the synthesized peptides were confirmed by mass spectrometry (major peak I + H^+: *m/z* 1054.3 – calc. *m/z* 1053; and major peak II + H^+: *m/z* 1067.5 – calc. *m/z* 1067).

2.2. Sample preparation

Peptide samples were prepared in two ways. (1) The preparations for the studies were preliminarily dissolved in 100% DMSO (with regard to the final concentration of 3–5%) and adjusted to the required concentration (0.2–2.0 mg/ml) with 5% acetic acid (pH 3.0). The dilution of the samples was performed on ice. (2) To obtain a monomer state of the peptides, the samples were preliminarily dissolved in ammonia (NH_4OH), the concentration was measured, and aliquots of the required concentration (0.4–0.7 mg/ml) were obtained and lyophilized. Prior to the experiment, the aliquots were dissolved in DMSO (the final concentration 5%), then adjusted to the final concentration 5% with acetic acid. The dilution of the samples was conducted on ice. For kinetic studies,

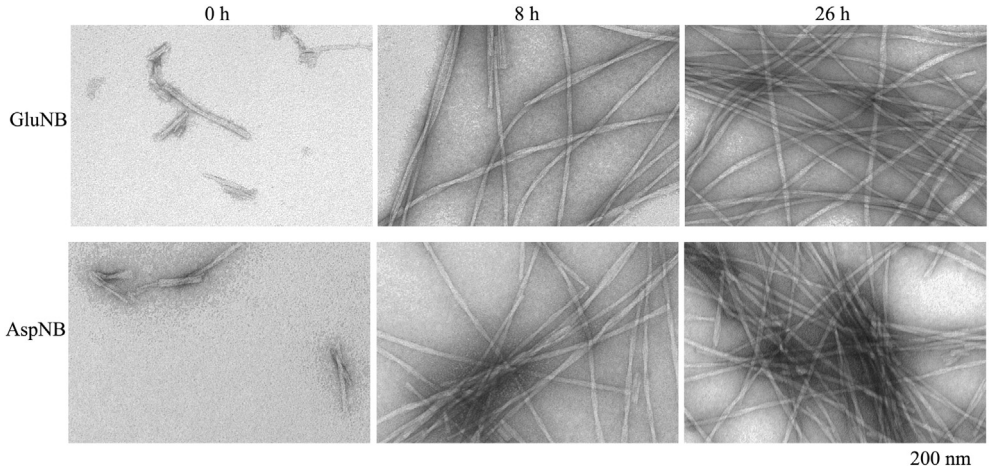

Fig. 1. Electron microscopy images of peptide preparations. EM images of preparations of peptides GluNB and AspNB at C = 0.2 mg/ml in 5% acetic acid (5% DMSO) at 37 °C in point "0" and after 8 h and 26 h incubation.

ThT was added to the final concentration 25 μM, while for the electron microscopy studies ThT was not added. Incubation of the preparations was carried out at 37 °C.

2.3. Electron microscopy (EM)

Prior to staining, the concentration of the samples was adjusted to 0.2 mg/ml. Copper grids (400 Mesh) coated with a Formvar film (0.2%) were mounted on a sample drop (10 μl) (upon preparation of gels, a sample drop was layered on top of the grid). After 5 min absorption, the grids with the preparations were negatively stained for 1.5–2.0 min with 1% (weight/volume) aqueous solution of uranyl acetate. The excess of the staining agent was removed with filter paper. Prior to staining, gel preparations were washed with 5% acetic acid for 30 s. The preparations were analyzed using a JEM-100C transmission electron microscope at the accelerating voltage of 80 kV. Images were recorded on the Kodak electron image film (SO-163) at nominal magnification of 40,000–60,000.

2.4. Fluorescence spectroscopy (FS): thioflavin T (ThT) fluorescence assay

Free ThT has excitation and emission maxima at 350 and 450 nm, respectively. Upon binding to fibrils, the excitation and emission λ_{max} values change to 450 and 485 nm, respectively. A stock solution of ThT was prepared at a concentration of 40 mM in 5% acetic acid (pH 3.0). For ThT fluorescence, aliquots of ThT were added to the peptide samples to achieve the final ThT concentration of 25 μM. ThT was present in the samples over the entire time of fibril formation (up to 100 h). Dilution of the samples was performed on ice. Fluorescence measurements were carried out using a Cary Eclipse fluorescence spectrophotometer (Varian, Australia) at 37 °C.

2.5. Molecular modeling

Structure 4UZR (chains A, B, C, D, E, F) from the Protein Data Bank was taken as a template to construct an arrangement of β-layers. Initially, fragments of amino acid residues from 79 to 84, 88 to 94, 97 to 102, 106 to 111, 116 to 121, 127 to 131, 134 to 138, 142 to 147 were taken from the pdb-file 4UZR. All these fragments correspond to the β-structure. β-Strands inside each β-layer were arranged antiparallel to each other. Using Molecular Dynamics simulations we demonstrated that such organization is the most stable in comparison with the parallel arrangement of β-strands (see the Data in Brief [21]). Using the YASARA program [22], two or three amino acid residues were added at the *N*- and *C*-termini of each β-strand. Then, the following amino acid sequences corresponding to two peptides V**D**SWNVLVAG (AspNB) and V**E**SWNVLVAG (GluNB) were fitted in each of these 48 β-strands. Thus, two structures that differ in amino acid sequences were obtained and minimized by the YASARA program. The principal geometric criterion of construction was the lack of steric overlaps between the van der Waals radii of the atoms.

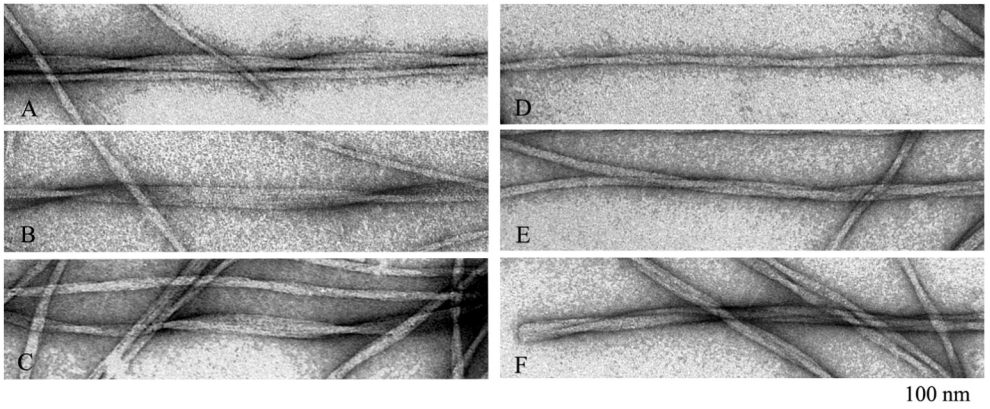

Fig. 2. Polymorphism of GluNB fibrils. Sample (0.2 mg/ml) in 5% acetic acid (5% DMSO) after 26 h incubation at 37 °C: fibrils in the form of twisted ribbon-like structures with periods of (A) 280 nm, (B) 500 nm, (C) 300 nm. Fibrils in the form of bundles of different diameters: (D) thin fibril with the diameter of about 15 nm in its wide part and 8 nm in its narrow part; (E) two fibrils transform into a wider fibril; (F) fibrils of different diameters. The widest fibril has the diameter of about 30 nm.

2.6. Mass spectrometry (MS)

The samples were dissolved in 30% acetonitrile containing 0.1% trifluoroacetic acid. The concentration of peptides was 0.1–0.3 mg/ml. The mass spectrometric analysis was performed with an Orbitrap Elite mass spectrometer (Thermo Scientific, Germany). The samples were ionized by nanoelectrospray, with a direct injection of the sample. An orbital trap with a resolution of 240,000 was used as a detector. The voltage supplied to the capillary varied from 0.8 to 1.5 kV. The mass spectrum was recorded in the range from 500 to 2000 *m/z*. To determine the mass of the substance by the value of its peak on the mass spectrum, it is necessary to multiply the *m/z* value by the charge value and subtract the mass of protons.

2.7. Determination of peptides involved in formation of amyloid fibrils

Mature fibrils of both peptides were obtained in the same way as for fluorescence studies (without ammonia pretreatment). The samples were pre-dissolved in 100% DMSO (the final concentration of 5%) and adjusted to the concentration of 0.6 mg/ml with 5% acetic acid (pH 3.0). The dilution of the samples was performed on ice. After dissolving, the samples were incubated for 24 h at 37 °C.

Centrifugation was used to isolate amyloid fibrils from monomer forms and oligomers. Then isolated fibrils were treated with a mixture of proteases (trypsin, chymotrypsin, and proteinase K). The proteases were added so that the ratio between the peptide and enzyme was 25:1. For supporting the activity of proteinase K, $CaCl_2$ was also added

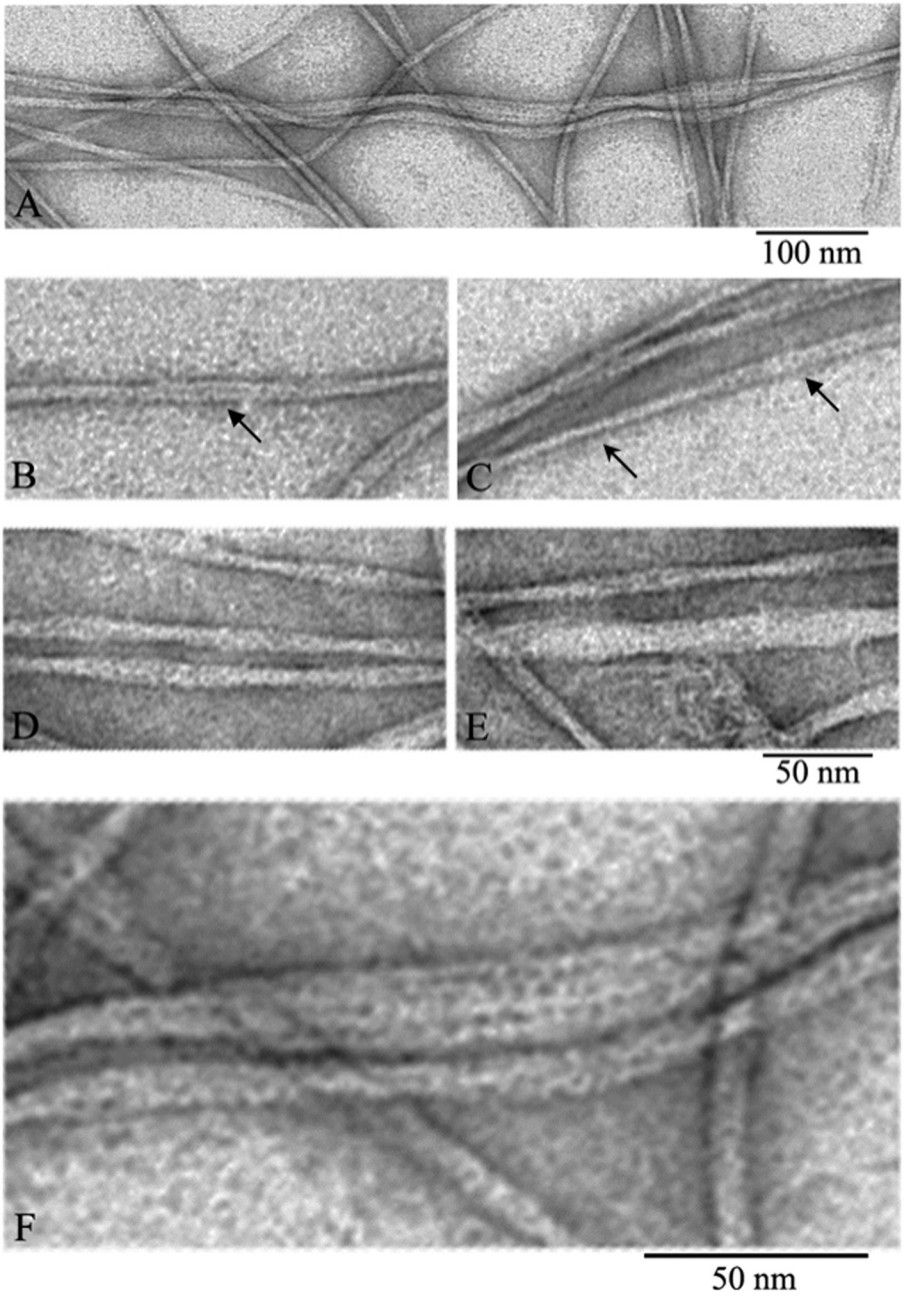

Fig. 3. EM images of field fragments and fibrils of peptide GluNB. Sample (0.2 mg/ml) in 5% acetic acid (5% DMSO) after 26 h incubation at 37C: (A) field fragment, (B) thin fibril with the diameter of about 6–8 nm; (C) thin fibril with the diameter of 6–8 nm in its wide part and 3–4 nm in its narrow part; (D, E) fibrils in the form of bundles of different diameters; (F) fibril fragment in the form of a bundle under high magnification.

to the final concentration of 5 mM. The fragments cleaved by the proteases were washed, and the remaining fragments included in fibril structures were pelleted once again and isolated. The conditions of limited proteolysis were chosen so that the monomer form would be completely degraded while the fibril moiety would retain long fragments. Then the isolated residual fibril structures were dried using a vacuum concentrator, after which they were dissolved in a small volume of formic acid and then in 10 mM ammonium acetate buffer.

The obtained set of peptides was analyzed by the method of tandem mass spectrometry. The peptides obtained after hydrolysis were separated by HPLC and analyzed by a high-performance mass spectrometer (Orbitrap Elite mass spectrometer, Thermo Scientific, Germany). Then the peptides were identified using the Peaks Studio 7.5 program (Bioinformatics Solution Inc., Canada). This program makes it possible not only to identify peptides but also to estimate their relative concentration in the probe. Peptides with the signal intensity over the ion flux in excess of 10^6 were considered significant.

2.8. X-ray diffraction

The peptides (C = 0.5 mg/ml) for X-ray diffraction analysis in 5% acetic acid (5% DMSO) were prepared after 48 h incubation at 37 °C (method (1)). The peptide samples were concentrated down to 5–10 mg/ml at room temperature using an Eppendorf 5301 vacuum concentrator. The peptides after ammonia treatment were concentrated by centrifugation at 12,000 rpm for 10 min at room temperature. Then the preparation droplets (about 6–7 μl) were placed within the space (about 1.5 mm) between the ends of glass tubes (rods) (about 1 mm in diameter) coated with wax [23]. The preparations were dried for several hours in Petri dishes. The fiber diffraction images were collected using a Microstar X-ray generator with HELIOX optics, equipped with a Platinum135 CCD detector (X8 Proteum system, Bruker AXS) at the Institute of Protein Research, RAS, Pushchino. Cu Kα radiation (λ = 1.54 Å) was used. The samples were positioned at the right angle to the X-ray beam using a 4-axis kappa goniometer.

3. Results and discussion

3.1. Electron microscopy for peptide samples prepared by method (1)

According to EM data, both peptides could form fibrils. Fig. 1 shows EM images of peptide preparations with C = 0.5 mg/ml at point "0" and after 8 h and 26 h incubation in 5% acetic acid (5% DMSO) at 37 °C.

Under these conditions, a small number of short fibrils frequently assembled in bundles are observed at point "0" (Fig. 1). As the time of incubation increased (8 h, 24 h), the number of bundles of short fibrils decreased, and the length of fibrils grew to several μm. Some fibrils of about 6–8 nm in diameter began interacting with each other forming fibril bundles or occasionally fibril ribbons of different widths. It should be noted that in 5% acetic acid (5% DMSO) the morphology of GluNB and AspNB peptides was similar, but the rate of fibril formation was higher for the AspNB peptide (see the binding with ThT below). After 48 h incubation, the gel-like transparent sediment was seen on the walls of the tubes (Fig. S1 from the Supplementary). In that case, as shown by the data of EM analysis, the number of fibrils became smaller, which was related with the formation of the gel-like sediment. When the concentration of the peptide was 1 mg/ml, the gel-like sediment was formed in 24 h incubation for GluNB and in 8 h for AspNB. At C = 2 mg/ml the gel-like sediment was formed within 1–2 h incubation for the both preparations.

A more detailed analysis of the morphology of fibrils of the both preparations revealed strong polymorphism of fibrils (Fig. 2). Fibrils could form ribbons of different widths. Such ribbons could be twisted and formed helices with different periods (Fig. 2A–C). Fibrils in the form of twisted bundles were most common. The diameter of the thinnest fibrils in the form of bundles was about 15 nm in their wide part and about 6–8 nm in the narrow part (Fig. 2D). Thin fibrils joined to each other forming bundles of different diameters (Fig. 2E, F). It can be seen on the preparation of peptide GluNB (Fig. 3) that the thinnest (single) fibrils have the diameter of about 6–8 nm and are formed of ring-like oligomer structures of the same diameter. When such a fibril was twisted, its diameter in the bending site was about 3–4 nm, which indicated implicitly the height of the fibril or the height of the ring oligomer (Fig. 3B, C). In that case, ring oligomers in the thin fibril either were joined ring-to-ring or were packed in a fibril slightly overlapping each other. The internal diameter of the ring oligomer was 2–3 nm. The same ring structures formed fibril bundles. In the latter case, the oligomers were packed randomly in the fibril (Fig. 3D–F).

It is remarkable that careful consideration allows spotting an interesting morphology of both peptides (Fig. 4): when thick fibrils were formed, frequently thin fibrils did not form second order helices but were packed closely joining to each other like two snakes having wave-like morphology.

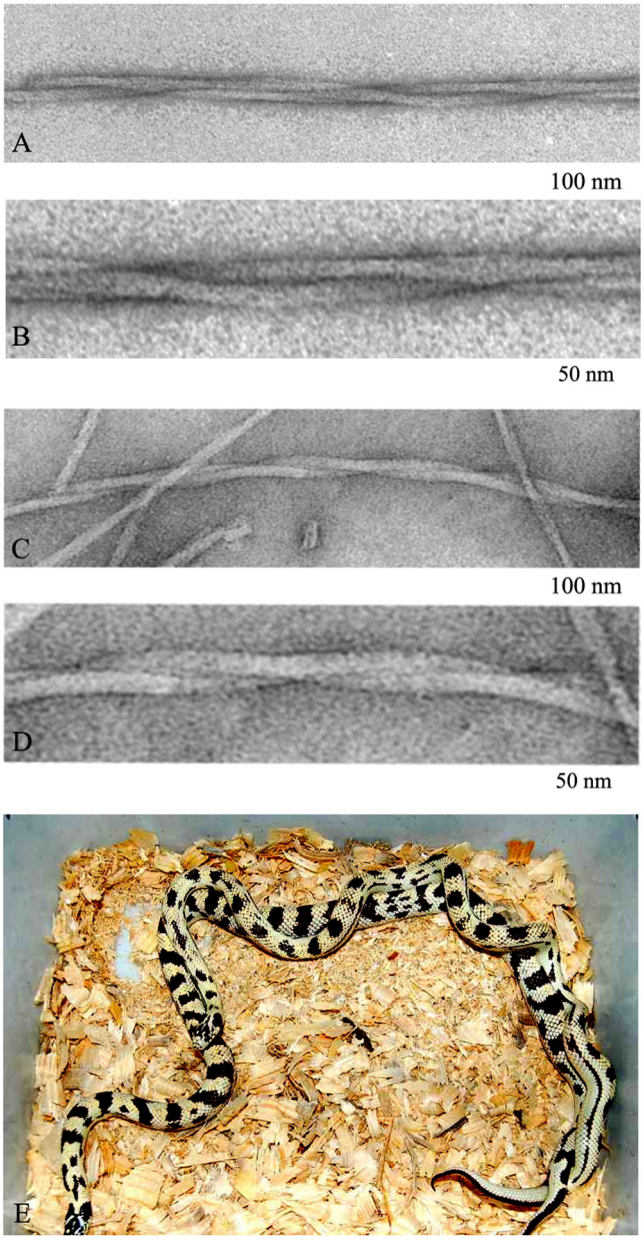

Fig. 4. New morphology of amyloid fibrils. EM images of preparations of GluNB and AspNB peptides (0.5 mg/ml) in 5% acetic acid (5% DMSO) after 26 h incubation at 37 °C. Wave-like fibrils lie close to each other: (A–B) GluNB; (C–D) AspNB; (E) intertwining of two snakes.

3.2. Electron microscopy for peptide samples prepared by method (2)

It was shown that even when AspNB and GluNB were incubated at C = 0.2 mg/ml it was not possible to reproduce the lag period by method (1). Ammonia was used to obtain a homogeneous monomer preparation of peptides [24], because method (1) did not allow achieving zero point in kinetic experiments. At the beginning of the incubation (zero point) short fibrils were observed with EM.

To perform EM studies, the samples treated with ammonia were prepared analogously to the samples prepared by method (1). Fig. 5 shows images of peptide preparations at C = 0.5 mg/ml after ammonia treatment in 5% acetic acid (5% DMSO) in point "0" and after 21 h incubation at 37 °C. The EM data show that at these concentrations a small number of short fibrils could be seen in point "0". After 30 h incubation there appeared a large number of mature fibrils of several μm long with different morphology. But it is worth noting that the morphology of GluNB and AspNB fibrils was different. Fibrils in the form of bundles of different thicknesses were most common for peptide GluNB (Fig. 6); they were similar to fibrils of peptide preparations not treated with ammonia. The diameter of the thinnest fibrils was about 6–8 nm (Fig. 6B). A fibril was formed of ring oligomers with the diameter of about 6–8 nm interacting with each other either ring-to-ring or slightly overlapping each other. Wider fibrils were also formed of ring oligomers, but the latter had no strict order upon interaction (Fig. 6C, D). Lateral association of fibrils was most common for peptide AspNB (Fig. 7). The thinnest fibrils also had the diameter of nearly 6–8 nm; such fibrils formed ribbons of different widths. In that case, single fibrils in ribbons could interact with each other either by side surfaces of ring oligomers (Fig. 7) (then the width of two fibrils would be about 15 nm) or by end faces (then the width of two fibrils would be about 8 nm) (Fig. 7C), which indicated indirectly to the height of a single fibril or a ring oligomer (about 3–4 nm). In ring oligomer structures it was possible to estimate approximately the internal diameter of the ring which was about 2–3 nm. However, in addition to fibrils in the form of ribbons (lateral association) there were also fibrils in the form of bundles of different diameters (Fig. 7D, E, F). Such morphology is characteristic of fibrils of peptides prepared without ammonia treatment and peptide GluNB treated with ammonia. As seen from Fig. 7E, F, fibrils in the form of bundles were also formed of ring oligomers with the diameter of about 6–8 nm interacting randomly with each other in fibrils. But it should be noted that for both ammonia treated peptides twisted fibrils occur infrequently, and what was more interesting, no fibrils with a new morphology were observed.

Thus, fibrils prepared using different methods can have different morphology. If peptides are not treated with ammonia (method (1)), there are fibrils of similar morphology; after ammonia treatment (method (2)) homologous peptides GluNB and AspNB form fibrils of different morphology. In addition to the effect of conditions of sample preparation on their morphology, there is a new morphology of fibrils, in which the diameter of fibrils increased not by simple twisting of thinner fibrils, but due to close interaction of two or more wave-like fibrils of a smaller diameter. In this case, if fibrils are packed side by side, a structure is formed resembling two snakes lying side by side. Such morphology may have been observed earlier, but it has not been described or reported.

3.3. Fluorescence spectroscopy (FS): thioflavin T (ThT) fluorescence assay

According to the FS data, the AspNB and GluNB peptide samples prepared by method (1) had no lag-period at concentration 0.5 mg/ml. Therewith, the intensity of ThT incorporation was higher in the AspNB peptide (Fig. 8). ThT fluorescence was absent in samples with concentration of 0.1–0.2 mg/ml.

Lag-periods were observed in the peptide samples prepared by method (2), at peptide concentrations from 0.4 to 0.55 mg/ml. No kinetics of ThT incorporation was observed at C = 0.3 mg/ml. But EM data showed that even in the presence of lag-periods it was possible to see a small number of fibrils in the "zero" point. The lag-period for the AspNB peptide (C = 0.5 mg/ml) was about 8 h, whereas for the GluNB peptide (C = 0.5 mg/ml) it was about 28 h (Fig. 9). According to the EM data, after 55 h incubation the number of fibrils for the AspNB preparation was larger than for the GluNB preparation (data not shown).

Unfortunately, it is difficult to reproduce the lag time period. However, the treatment with ammonia actually could slow the process of fibril formation, indicating that in the initial period of their formation the number of monomers in peptide samples was significant.

To analyze the size of nuclei of amyloid fibril nucleation, formed by the given peptides, the theoretical approach developed earlier [25] was used. According to this approach, for estimation of the size of fibril

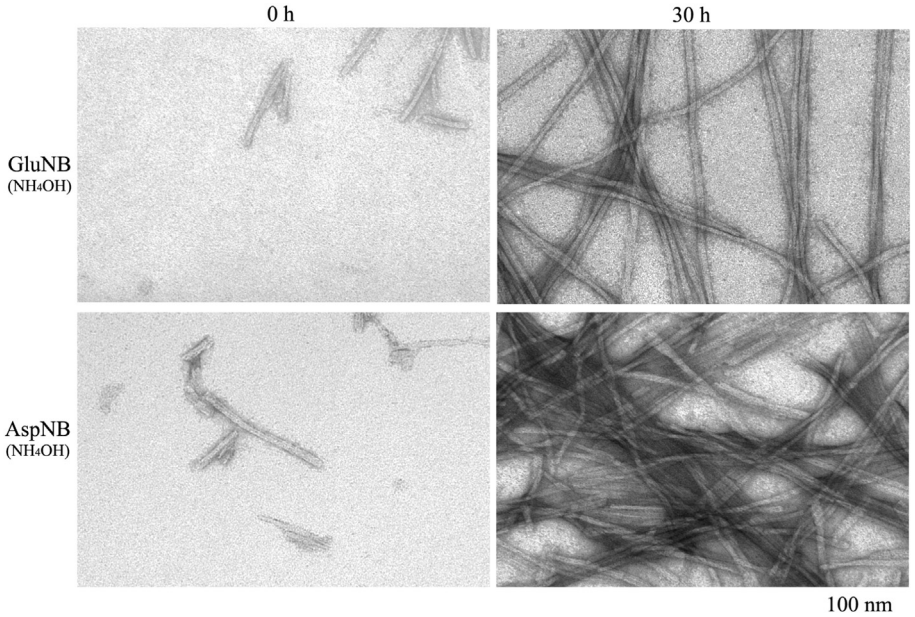

Fig. 5. EM images of preparations of GluNB and AspNB peptides preliminarily treated with ammonia. Samples (0.4 mg/ml) in 5% acetic acid (5% DMSO) and incubation at 37 °C in point "0" and after 30 h of incubation.

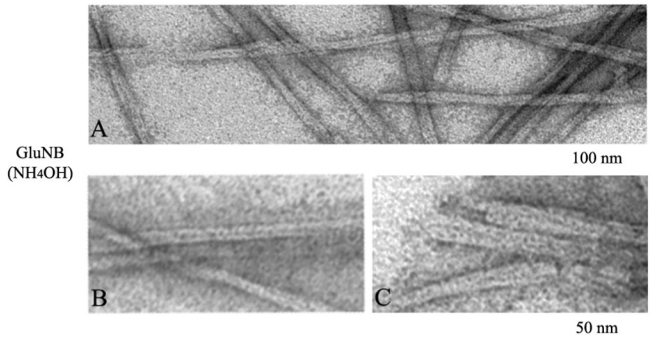

Fig. 6. EM images of field fragments and fibrils of ammonia treated preparation GluNB. Sample (0.4 mg/ml) in 5% acetic acid (5% DMSO) and incubation at 37 °C during 30 h: (A) field fragment, (B) a single fibril of 6–8 nm in diameter; (C) fragments of fibrils in the form of bundles.

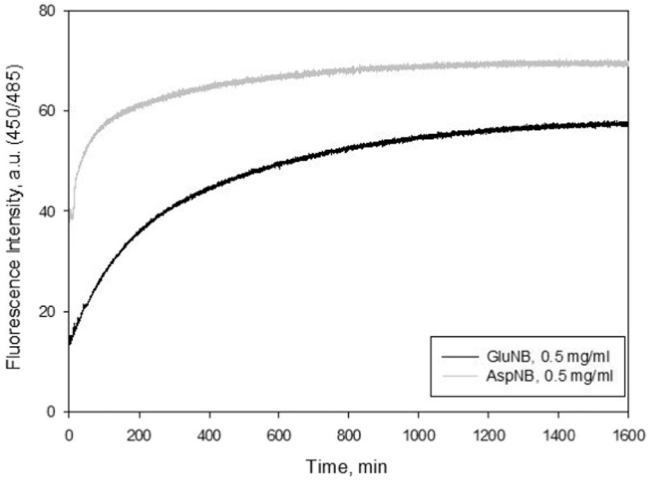

Fig. 8. Kinetics of ThT incorporation for AspNB and GluNB preparations of peptides at C = 0.5 mg/ml.

nuclei (the most unstable state on the monomer fibril pathway) and a possible scenario of fibril formation, it is necessary to perform a number of kinetic experiments, where the only variable parameter is the concentration of monomers. Characteristic times T_{lag} (the lag-time), T_2

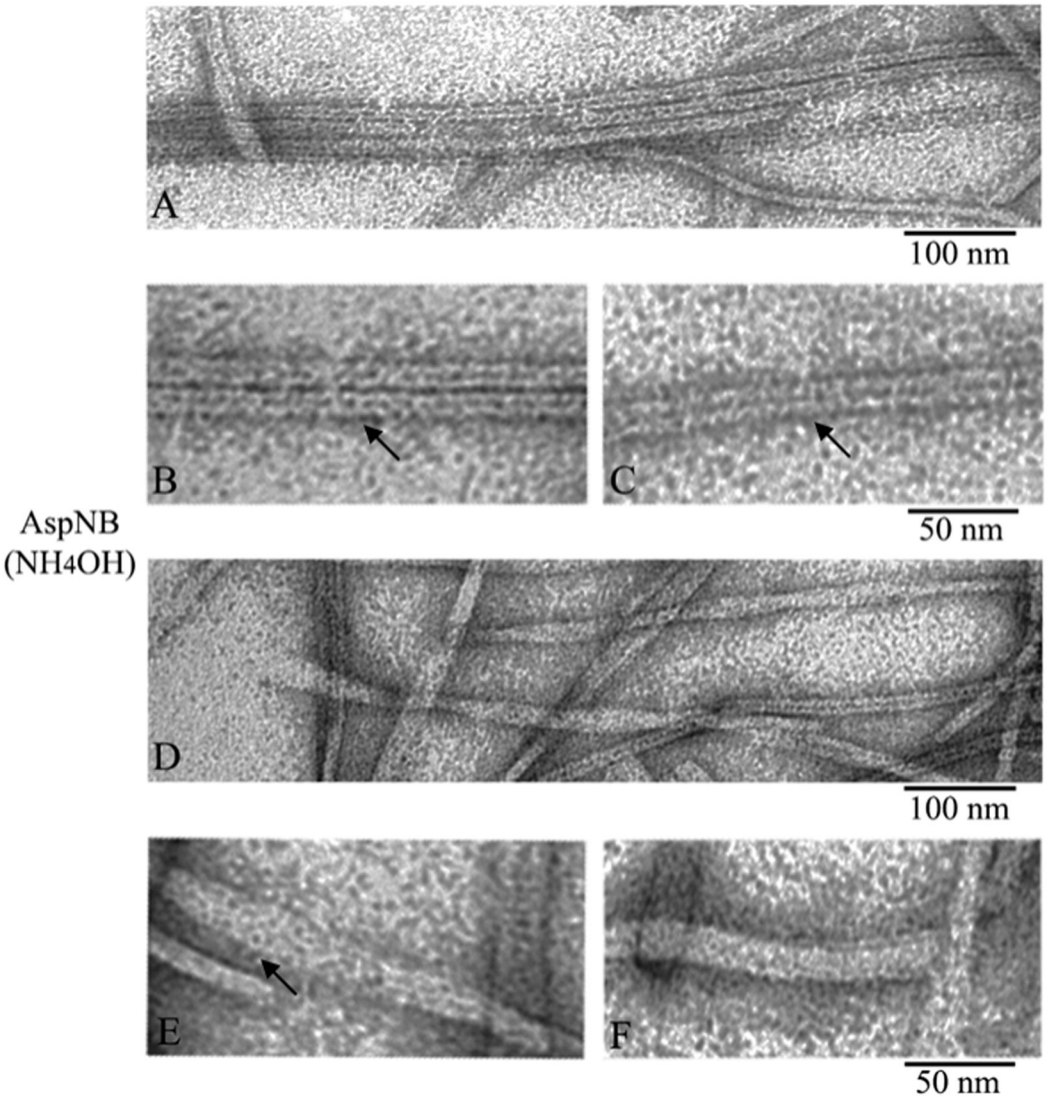

Fig. 7. EM images of field fragments and fibrils of ammonia treated preparation AspNB. Sample (0.4 mg/ml) in 5% acetic acid (5% DMSO) and incubation at 37 °C during 30 h: (A) lateral association of fibrils in the form of a wide ribbon; (B) two fibrils associated by their side surfaces; (C) two fibrils contact the Formvar support by their side surfaces; (D) field fragment with fibrils in the form of bundles; (E, F) fragments of fibrils in the form of bundles. Ring oligomers associate randomly (E, arrow).

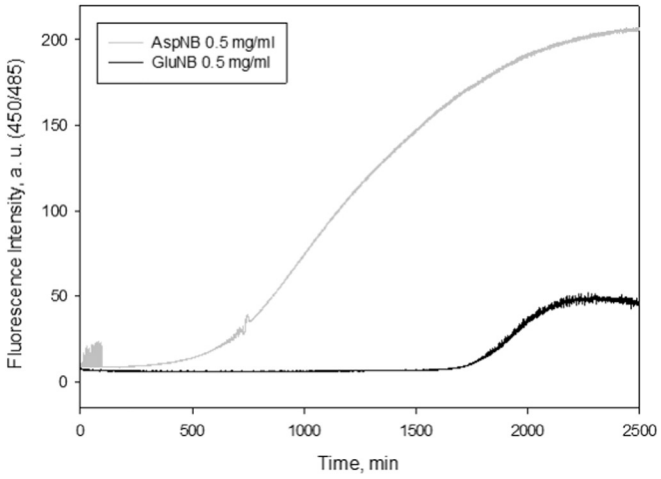

Fig. 9. Kinetics of ThT incorporation for AspNB and GluNB preparations of peptides at C = 0.5 mg/ml. The samples were preliminarily dissolved in ammonium hydrate.

Fig. 11. Tandem mass spectrometry analysis. Fragments (shown as blue bands) of AspNB (A) and GluNB (B) identified by Peaks Studio 7.5 after limited proteolysis and tandem mass spectrometry of fibrils from these peptides. Small letter "s" stands for "sodium" and means that this fragment has sodium adducts. Small letter "f" stands for formylation of an amino acid residue. These modifications were induced by the conditions of the experiment.

(the time of transition of all monomers into an aggregate) and L_{rel} (the T_{lag}/T_2 ratio) are calculated for each curve obtained in the experiments. It has been shown [14] that dependences of $\ln T_2$ and L_{rel} versus $\ln[M_\Sigma]$ (the logarithm of the initial concentration of monomers) is linear, and the values of corresponding coefficients of the slope for each dependence can be used for computation of the size of fibril nuclei and identification of the mechanism of aggregate formation.

It was found that the scenario of growth of amyloids, formed by these peptides, was exponential, i.e. in addition to the formation of nuclei of primary nucleation, nuclei of secondary nucleation were also formed by the branching mechanism that accelerated generation of new fibrils. As shown by our calculations, the size of the nuclei of secondary nucleation n_2 was 1.96 ± 3.89 (see Supplementary Fig. S2), and that of the primary nucleation is 3.46 ± 5.70. The errors are too large to make any conclusion on the sizes of nuclei.

3.4. X-ray diffraction analysis

As the data from X-ray diffraction analysis showed, the samples of GluNB and AspNB peptides yielded a diffraction pattern with specific reflections for the cross-β structure (Fig. 10). The GluNB sample had reflections of 4.6 Å, which correspond to the distance between β-regions, and 9.2 Å (diffusion), thus indicating that the distance between β-sheets and the AspNB sample was correspondingly 4.6 Å and 9.0 Å (Fig. 10B, C). Additional reflections are summarized in Supplementary Table S1.

It should be noted that for both peptides, there were characteristic reflections for the cross-β structure but they were not perfect (Fig. 10A). This showed that either the fibrils in the sample were insufficiently well oriented or the cross-β structure in the fibrils was not ideal.

The presence of reflections on the meridian to 2 Å indicates that the individual fibrils have highly ordered internal structures along the fiber axis. The 2.8 Å reflection on the meridian is the harmonic of the 4.76 reflection (see Supplementary Fig. S3 and Supplementary Table S2). Reflections with spacings of 2.90 to 2.39 correspond to the 40–48 order, suggesting that the amyloid core contains 40–48 beta-strands (see Table 2 in [26]). Table 1 in paper [27] summarizes Bragg spacings for fragments of the Aβ peptide. The meridional reflection at 53 Å indicates a periodic structure along the H-bonding direction. Models that could account for the low-angle meridional reflections in Aβ peptides 9–28 and 1–40 are (a) a periodic arrangement of discrete objects along the fibril axis, (b) a staggered arrangement of subfibrils, and (c) twisting of the fibril. Case (a) supports our model both for Aβ40 [19] and for the short peptide of 10 residues long.

For fragment Aβ(1–28) a series of small-angle, equatorial maxima were consistent with a tubular fibril having a mean diameter of 86 Å and a wall composed of pairs of cross-β pleated sheets. The data may also be consistent with pairs of cross-β sheets that are centered 71-Å apart [28]. Reflections with spacings 15–25 Å can correspond to the hollow in our tubular cylinder. As our generator has no possibility to obtain low-angle reflections we cannot obtain the reflection with spacings 30–70 Å.

An interesting result of X-ray analysis for fragments of Aβ peptides of a similar length for our peptides (18–28, 17–28, 15–28) should be mentioned [27]. Equatorial reflections are indexed one dimensionally

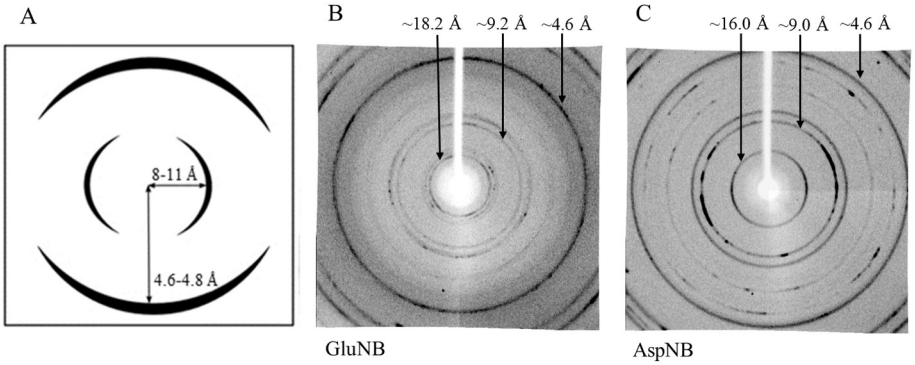

Fig. 10. X-ray diffraction patterns of GluNB and AspNB peptides. Peptides were prepared in 5% acetic acid (5% DMSO, pH 3.0). The peptide samples were concentrated down to 5–10 mg/ml at room temperature using an Eppendorf 5301 vacuum concentrator. A) Schematic image of a typical diffraction picture of well oriented amyloid fibrils. The reflection of 4.6–4.8 Å corresponds to the distance between β-regions, and the reflection of 8.0–11.0 Å indicates the distance between β-sheets; B) GluNB; C) AspNB.

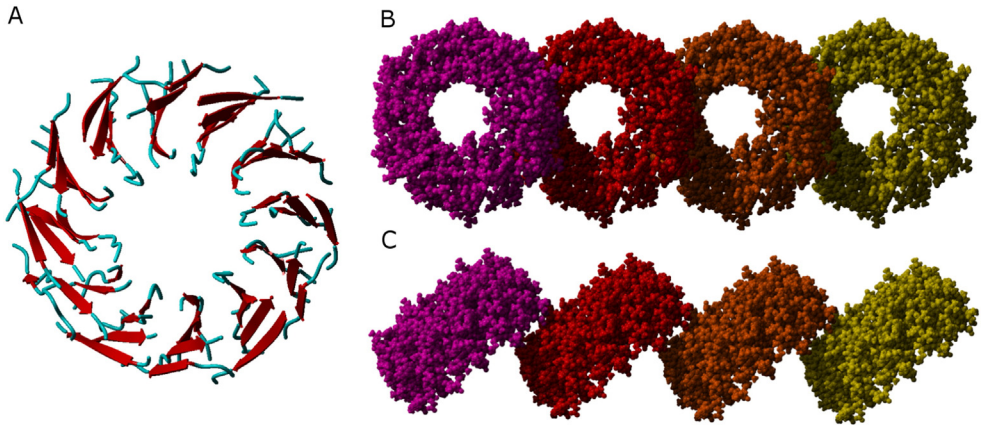

Fig. 12. Molecular modeling of amyloid fibrils of AspNB peptide. (A) Fragments from amino acid residue 79 to 84, 88 to 94, 97 to102, 106 to 111, 116 to 121, 127 to 131, 134 to 138, 142 to 147 were taken from pdb-file 4UZR. All these fragments correspond to the β-structure (red color). Using the YASARA program, two or three amino acid residues were added at the *N*- and *C*-termini of each β-strand. The AspNB peptide was fitted in each of these 48 β-strands. (B–C) Molecular structure for amyloid fibrils formed by AspNB. (B) Top and (C) side view of organization of ring-like oligomer structures of amyloid fibrils. The diameter of the hole of a ring is about 2 nm, the width of the ring is about 2 nm, and the height is about 3 nm.

with periods of 38, 37, and 40 Å for peptides 18–28, 17–28, and 15–28, respectively. The intensity diminished between 1/40 and 1/20 Å, suggesting that ~30 Å thick plates are stacked with a 40 Å period. This size corresponds to β-strands that are 10 residues long in the chain direction.

Summarizing the above facts we can make the following conclusion. According to the literature data for peptides of a similar length, in our model we have tubular cylinders which are stacked with a 40 Å period, which corresponds to our model distance (see Section 3.6). The tubular cylinder includes more than 40 β-strands, has a hollow with the diameter of ~20 Å. This indirectly implies that the general statement about the formation of elongated β-sheets in fibrils as long as the fibril itself was not strictly proven.

3.5. Determination of regions involved in the amyloid fibrils

The tandem mass spectrometry analysis revealed that after 1 h of treatment with proteases part of AspNB was inaccessible for proteases and predominantly covered the whole sequence of the peptide. However, there was also a fragment lacking two *N*-terminal amino acid residues (valine and aspartate), but this fragment had a smaller automatically calculated reliability score. This result was also the same after 8 h of proteases treatment (Fig. 11A). As for GluNB, both after 1 h and 8 h incubation with proteases the identified fragment covered the whole sequence of the peptide (Fig. 11B).

3.6. Molecular structure of amyloid fibrils formed with AspNB and GluNB

The most remarkable was that high magnification of EM images allows us to reveal that the thinnest amyloid fibrils were formed of ring structures with the diameter of about 6 nm (Figs. 5, 6) packed either directly ring-to-ring, or ring-on-ring with a slight shift. We suggested a molecular structure for this type of arrangement of oligomer structures. According to EM images, the diameter of the hole of a ring was about 2 nm, the width of the ring was about 2 nm, and the height was about 3 nm. 48 β-strands were organized in the oligomer structure, in which β-strands inside each β-layer were arranged antiparallel to each other (Fig. 12A). Such organization was the most stable in comparison with

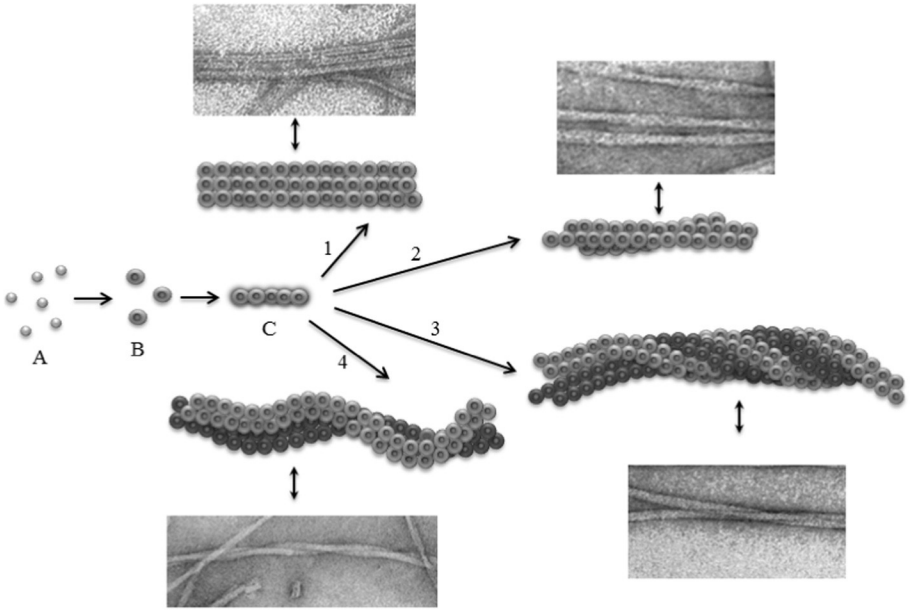

Fig. 13. Schematic representation of the fibril polymorphism. (A) Monomers; (B) oligomers; (C) single fibril. The formation from oligomers: 1, ribbons; 2, thin bundles; 3, large diameter bundles; 4, new morphology of amyloid fibrils.

the parallel arrangement of β-strands (see the Data in Brief [21]). Four ring-like oligomer structures with amino acid sequence V**D**SWNVLVAG were constructed manually (Fig. 12B, C).

The content of β-structure is practically the same after 3 ns molecular dynamics simulations (see Supplementary Table S3). The X-ray analysis of our peptides and of the fragments of Aβ peptides of similar length (18–28, 17–28, 15–28) supports our model that we have tubular cylinders with a hollow about 20 Å, which are stacked with a 40 Å period. Moreover, the tandem mass spectrometry analysis also supported our molecular structure.

4. Conclusions

EM data allows us to conclude that the preparations of amyloidogenic GluNB and AspNB peptides can form fibrils of up to several micrometers long. Under the same conditions, fibrils of different morphologies are formed, i.e. pronounced polymorphism of mature fibrils is observed. Polymorphism of both GluNB and AspNB is similar, i.e. substitution of Glu for Asp in the second position does not affect the morphology of the formed fibrils as is shown by EM data. At the same time, the results of EM and fluorescence analysis demonstrate that the process of fibril formation for peptide AspNB goes faster.

However, after ammonia treatment, the substitution of Glu for Asp leads to a change in the morphology of fibrils of homologous peptides. In the GluNB peptide, mainly bundles of different diameters are formed, while in the AspNB, peptide fibrils in the form of ribbons of different widths are more frequent than bundle fibrils. Thus, the most characteristic is the lateral association of single fibrils. Here, the same as for the sample prepared by method (1), the process of fibril formation for AspNB is faster and more intense as is shown by the data from the fluorescence analysis.

With this study of the formation of fibrils in GluNB and AspNB (method (1)), we are the first to describe the new morphology of fibrils when fibrils increase in their diameter not due to association of thinner fibrils with their twisting relative or due to lateral association, but due to close interaction of two or more wave-like fibrils of a smaller diameter. In this case, a structure resembling two snakes lying side by side is formed. Such morphology may have been observed previously, but it has not been specially denoted and described.

The most essential result from the EM studies is that in spite of strong polymorphism of fibrils, in all cases the main starting element of a fibril (its building unit) of any morphology is a ring oligomer with the external diameter of about 6–8 nm, the internal diameter (of the hole) of about 2–3 nm and the height of about 3–4 nm (estimated by the bending sites of a single fibril, Fig. 3B, C). At the initial stage of fibril formation such oligomers associate with each other either ring to ring or slightly overlaying each other. In this case, thin fibrils of 6–8 nm in diameter are formed. Under prolonged incubation, fibrils of several micrometers long and with different morphology are formed. Single fibrils can associate with each other forming ribbons of different widths or bundles. Bundles can have different diameters because of random sticking of ring oligomers or various interactions of bundles with each other. In both cases, the diameters of fibrils increase. These data correspond with our previous results from the EM studies of fibrils formed by insulin and Aβ peptide [18–20].

It should be noted that the data from X-ray analysis show that fibrils formed from ring oligomers have a cross-β structure. This is consistent with our proposed model of oligomer structure and the suggested mechanism of packing of oligomers in fibrils. According to the proposed model the ring-like oligomer includes β-strands as well as 12 β-sheets (Fig. 12A). This quantity is sufficient to produce the characteristic reflections for cross-β structure.

According to a simplified scheme, the formation of fibrils happens as follows: a monomer → a destabilized monomer → an oligomer → a fibril. The weakest point in this scheme is an oligomer. For many amyloidogeneic proteins or peptides, oligomers can be observed at the initial stage of fibril formation; oligomers (Aβ peptides, insulin) frequently have ring morphology [18–20]. It is unclear what occurs at the stage 'an oligomer → a fibril'. In what way are fibrils formed from ring-like oligomers? We believe an oligomer is quite probable to be the basic unit of a fibril. Ring-like oligomers can form any morphology of a fibril, i.e. under certain conditions polymorphism of fibrils of the same preparation can be explained by different ways of interaction of oligomers (see Fig. 13). It is simpler to explain also the changes in morphology of fibrils even upon changes in different conditions of fibril formation (pH, ionic strength, temperature etc.). The effect of selective substitutions in the amino acid sequence of proteins or peptides on the change in the morphology of the formed fibrils becomes clearer.

Conflict of interest

We have no conflict of interests.

Transparency document

The Transparency document associated with this article can be found, in the online version.

Acknowledgments

We are grateful to T.B. Kuvshinkina for assistance in preparation of the manuscript. The studies were supported by the Russian Science Foundation (No. 14-14-00536).

Appendix A. Supplementary data

Supplementary data to this article can be found online at http://dx.doi.org/10.1016/j.bbapap.2016.08.002.

References

[1] F. Chiti, C.M. Dobson, Protein misfolding, functional amyloid, and human disease, Annu. Rev. Biochem. 75 (2006) 333–366, http://dx.doi.org/10.1146/annurev.biochem.75.101304.123901.
[2] M. Sunde, C. Blake, The structure of amyloid fibrils by electron microscopy and X-ray diffraction, Adv. Protein Chem. 50 (1997) 123–159.
[3] D.M. Fowler, A.V. Koulov, C. Alory-Jost, M.S. Marks, W.E. Balch, J.W. Kelly, Functional amyloid formation within mammalian tissue, PLoS Biol. 4 (2006), e6, http://dx.doi.org/10.1371/journal.pbio.0040006.
[4] F. Shewmaker, R.P. McGlinchey, R.B. Wickner, Structural insights into functional and pathological amyloid, J. Biol. Chem. 286 (2011) 16533–16540, http://dx.doi.org/10.1074/jbc.R111.227108.
[5] S.K. Maji, M.H. Perrin, M.R. Sawaya, S. Jessberger, K. Vadodaria, R.A. Rissman, P.S. Singru, K.P.R. Nilsson, R. Simon, D. Schubert, D. Eisenberg, J. Rivier, P. Sawchenko, W. Vale, R. Riek, Functional amyloids as natural storage of peptide hormones in pituitary secretory granules, Science 325 (2009) 328–332, http://dx.doi.org/10.1126/science.1173155.
[6] T.S. Kalebina, T.A. Plotnikova, A.A. Gorkovskii, I.O. Selyakh, O.V. Galzitskaya, E.E. Bezsonov, G. Gellissen, I.S. Kulaev, Amyloid-like properties of *Saccharomyces cerevisiae* cell wall glucantransferase Bgl2p: prediction and experimental evidences, Prion. 2 (2008) 91–96.
[7] E.E. Bezsonov, M. Groenning, O.V. Galzitskaya, A.A. Gorkovskii, G.V. Semisotnov, I.O. Selyakh, R.H. Ziganshin, V.V. Rekstina, I.B. Kudryashova, S.A. Kuznetsov, I.S. Kulaev, T.S. Kalebina, Amyloidogenic peptides of yeast cell wall glucantransferase Bgl2p as a model for the investigation of its pH-dependent fibril formation, Prion. 7 (2013) 175–184, http://dx.doi.org/10.4161/pri.22992.
[8] S. Tzotzos, A.J. Doig, Amyloidogenic sequences in native protein structures, Protein Sci. Publ. Protein Soc. 19 (2010) 327–348, http://dx.doi.org/10.1002/pro.314.
[9] H. Inouye, D.A. Kirschner, X-ray fiber and powder diffraction of PrP prion peptides, Adv. Protein Chem. 73 (2006) 181–215, http://dx.doi.org/10.1016/S0065-3233(06)73006-6.
[10] M.R. Sawaya, S. Sambashivan, R. Nelson, M.I. Ivanova, S.A. Sievers, M.I. Apostol, M.J. Thompson, M. Balbirnie, J.J.W. Wiltzius, H.T. McFarlane, A.Ø. Madsen, C. Riekel, D. Eisenberg, Atomic structures of amyloid cross-beta spines reveal varied steric zippers, Nature 447 (2007) 453–457, http://dx.doi.org/10.1038/nature05695.
[11] N. Sánchez de Groot, I. Pallarés, F.X. Avilés, J. Vendrell, S. Ventura, Prediction of "hot spots" of aggregation in disease-linked polypeptides, BMC Struct. Biol. 5 (2005) 18, http://dx.doi.org/10.1186/1472-6807-5-18.
[12] N.V. Dovidchenko, O.V. Galzitskaya, Computational approaches to identification of aggregation sites and the mechanism of amyloid growth, Adv. Exp. Med. Biol. 855 (2015) 213–239, http://dx.doi.org/10.1007/978-3-319-17344-3_9.

[13] S. Giannattasio, N. Guaragnella, M. Corte-Real, S. Passarella, E. Marra, Acid stress adaptation protects *Saccharomyces cerevisiae* from acetic acid-induced programmed cell death, Gene 354 (2005) 93–98, http://dx.doi.org/10.1016/j.gene.2005.03.030.
[14] P. Ludovico, M.J. Sousa, M.T. Silva, C. Leão, M. Côrte-Real, *Saccharomyces cerevisiae* commits to a programmed cell death process in response to acetic acid, Microbiol. Read. Engl. 147 (2001) 2409–2415, http://dx.doi.org/10.1099/00221287-147-9-2409.
[15] R.M. de Lucena, C. Elsztein, W. de Barros Pita, R.B. de Souza, S. de Sá Leitão Paiva Júnior, M.A. de Morais Junior, Transcriptomic response of *Saccharomyces cerevisiae* for its adaptation to sulphuric acid-induced stress, Antonie Van Leeuwenhoek 108 (2015) 1147–1160, http://dx.doi.org/10.1007/s10482-015-0568-2.
[16] N. Guaragnella, L. Antonacci, S. Passarella, E. Marra, S. Giannattasio, Achievements and perspectives in yeast acetic acid-induced programmed cell death pathways, Biochem. Soc. Trans. 39 (2011) 1538–1543, http://dx.doi.org/10.1042/BST0391538.
[17] O.M. Selivanova, M.Y. Suvorina, N.V. Dovidchenko, I.A. Eliseeva, A.K. Surin, A.V. Finkelstein, V.V. Schmatchenko, O.V. Galzitskaya, How to determine the size of folding nuclei of protofibrils from the concentration dependence of the rate and lag-time of aggregation. II. Experimental application for insulin and LysPro insulin: aggregation morphology, kinetics, and sizes of nuclei, J. Phys. Chem. B 118 (2014) 1198–1206, http://dx.doi.org/10.1021/jp4083568.
[18] N.V. Dovidchenko, A.V. Glyakina, O.M. Selivanova, E.I. Grigorashvili, M.Y. Suvorina, U.F. Dzhus, A.O. Mikhailina, N.G. Shiliaev, V.V. Marchenkov, A.K. Surin, O.V. Galzitskaya, One of the possible mechanisms of amyloid fibrils formation based on the sizes of primary and secondary folding nuclei of Aβ40 and Aβ42, J. Struct. Biol. 194 (2016) 404–414, http://dx.doi.org/10.1016/j.jsb.2016.03.020.
[19] E.I. Grigorashvili, O.M. Selivanova, N.V. Dovidchenko, U.F. Dzhus, A.O. Mikhailina, M.Y. Suvorina, V.V. Marchenkov, A.K. Surin, O.V. Galzitskaya, Determination of size of folding nuclei of fibrils formed from recombinant Aβ(1–40) peptide, Biochem. Biokhimiĭa 81 (2016) 538–547, http://dx.doi.org/10.1134/S0006297916050114.
[20] O.V. Selivanova, M.Y. Suvorina, A.K. Surin, N.V. Dovidchenko, O. Galzitskaya, Insulin and lispro insulin: what is common and different in their behavior? Curr. Protein Pept. Sci. (2016).
[21] A.V. Glyakina, N.K. Balabaev, O.V. Galzitskaya, Multiple unfolding intermediates obtained by molecular dynamic simulations under stretching for immunoglobulin-binding domain of protein G, Open Biochem. J. 3 (2009) 66–77, http://dx.doi.org/10.2174/1874091X00903010066.
[22] E. Krieger, G. Koraimann, G. Vriend, Increasing the precision of comparative models with YASARA NOVA—a self-parameterizing force field, Proteins 47 (2002) 393–402.
[23] L.C. Serpell, P.E. Fraser, M. Sunde, X-ray fiber diffraction of amyloid fibrils, Methods Enzymol. 309 (1999) 526–536.
[24] T.M. Ryan, J. Caine, H.D.T. Mertens, N. Kirby, J. Nigro, K. Breheney, L.J. Waddington, V.A. Streltsov, C. Curtain, C.L. Masters, B.R. Roberts, Ammonium hydroxide treatment of Aβ produces an aggregate free solution suitable for biophysical and cell culture characterization, PeerJ. 1 (2013), e73, http://dx.doi.org/10.7717/peerj.73.
[25] N.V. Dovidchenko, A.V. Finkelstein, O.V. Galzitskaya, How to determine the size of folding nuclei of protofibrils from the concentration dependence of the rate and lag-time of aggregation. I. Modeling the amyloid protofibril formation, J. Phys. Chem. B 118 (2014) 1189–1197, http://dx.doi.org/10.1021/jp4083294.
[26] M. Sunde, L.C. Serpell, M. Bartlam, P.E. Fraser, M.B. Pepys, C.C. Blake, Common core structure of amyloid fibrils by synchrotron X-ray diffraction, J. Mol. Biol. 273 (1997) 729–739, http://dx.doi.org/10.1006/jmbi.1997.1348.
[27] H. Inouye, P.E. Fraser, D.A. Kirschner, Structure of beta-crystallite assemblies formed by Alzheimer beta-amyloid protein analogues: analysis by X-ray diffraction, Biophys. J. 64 (1993) 502–519, http://dx.doi.org/10.1016/S0006-3495(93)81393-6.
[28] D.A. Kirschner, H. Inouye, L.K. Duffy, A. Sinclair, M. Lind, D.J. Selkoe, Synthetic peptide homologous to beta protein from Alzheimer disease forms amyloid-like fibrils in vitro, Proc. Natl. Acad. Sci. U. S. A. 84 (1987) 6953–6957.